Impact of motion correction on the quantitative analysis of DCE-MR Images

K. Rao[1], G. Jia[2], J. Heverhagen[2], R. Machiraju[1], J. Saltz[3], and M. Knopp[2]

[1]Computer Science and Engineering, [2]Biomedical Informatics, [3]Radiology The Ohio State University, Columbus, Ohio, USA
kishore@bmi.osu.edu

Abstract. Dynamic magnetic resonance imaging (DCE-MRI) carried out with contrast media such as Gd-chelate complex (Gd-DTPA) allows the non-invasive assessment of microcirculatory characteristics of malignant lesions. Quantitative estimation of lesion parameters from the passage of the contrast media requires the use of pharmacokinetic two-compartment model. The input to the model is the time-intensity plot from a region of interest (ROI) covering the lesion extent. The lengthy imaging process, elasticity of the organs and patient movement result in complex deformations in the subject requiring 3D motion correction for ROI alignment. This paper presents results on applying the Thirion Demon's 3D elastic matching procedure in the ITK framework on the two-compartment lesion parameters. Registration, meanwhile involves interpolation and smoothing operations thereby affecting the time-intensity plots. We explore the trade-offs that arise between registration and lesion parameter estimation. Experiments on synthesized and real deformation are presented.

1 Introduction

In oncological imaging, magnetic resonance imaging (MRI) allows for considerable tissue characterization based on its proton/water or fatty tissue content. Therefore, a three dimensional delineation of the lesion morphology is achieved. Meanwhile, the clinical implementation of functional assessment techniques such as the dynamic contrast-enhanced MRI (DCE-MRI) [1] have resulted in major advances in oncological applications. DCE-MRI allows for the non-invasive imaging of therapy response and diagnosis for the functional characterization of lesions [2].

DCE-MRI is achieved through the acquisition of sequential MRI images during the passage of a contrast agent through the tissue of interest. Intravenously injected extracellular contrast such as the Gadolinium chelate agents (Gd-DPTA) have been essential for the detection and delineation of tumors. Owing to their small molecular size, the contrast permits the characterization of lesion vasculature by diffusing and re-diffusing back through the altered capillary wall. Recent studies also show that the changes in signal intensity within a tumor reflects its angiogenic properties [1]. The quantification of the temporal

intensity signal in the tumor region relates to its vascular density and the rate of enhancement characterizes the arrangement and functional permeability within [3].

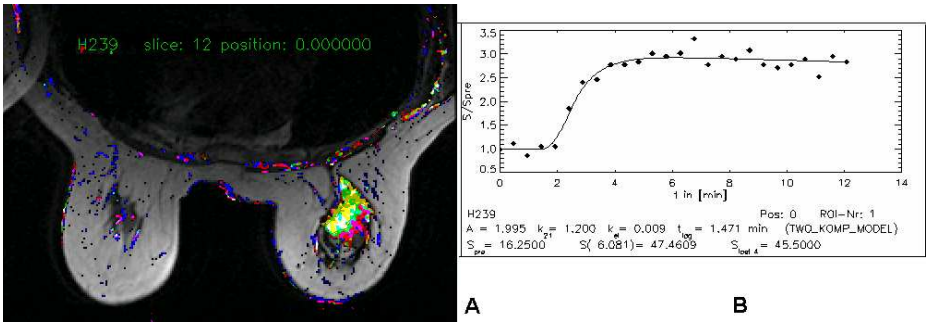

Fig. 1. A: Monitoring evaluation by DCE-MRI in a patient with invasive ductal carcinoma in the breast. The tumor ROI (A) reveals strong and intense enhancement with a typical time-intensity curve (B).

The pharmacokinetic two-compartment model describes the diffusion process of the contrast agent. The input is the temporal signal intensity observable from a suitably selected region-of-interest (ROI) encompassing an entire or portion of the lesion. The output of the model is composed of parameters of the intensity time curve. Model parameters are computed that can be used to relate to the lesion specific physiological concepts as shown in Figure 1.

Image acquisition in DCE-MRI involves 20-32 time-points each containing about 14-32 transversal slices of a 3D volume. The challenging aspect in quantification is the positioning of the ROI consistently to cover a lesion across all the epochs. The time required for imaging usually allows considerable motion by subject movement. While stationary organs like the central nervous system, bone marrow, the musculoskeletal system and the breast are more readily imaged, organs such as kidney, liver and lung can be burdened by motion artifacts. Further, organs such as the female breast are scanned in a pendant position and therefore amenable to non-linear deformation. Involuntary movement such as rolling of the patient, breathing, gravitation effects also cause motion [3].

Therefore, quantification of DCE-MRI data requires elastic 3D motion-correction procedures. Improper placement of the ROI in the motion affected time-points can affect the correct evaluation of the lesion parameters and hence its functional assessment. However, co-registration is also concomitant with image transformations leading to interpolation of the image field on a grid. Interpolation is akin to a low-pass filtering operation and hence pixel intensities are affected. Reduction in pixel intensities affect the amplitude, rise and wash-in or wash-out gradients of the time-intensity curves and hence the parameters.

In this paper, we describe the improvement in lesion parameter estimation as a result of using motion correction through the Thirion's demons registration method [4]. We especially explore artifacts of registration such as intensity smoothing in images and propose corrections. We present the comparative evaluation of the impact of registration parameters settings on the lesion pharmacokinetic parameter estimations. Experiments are performed using stationary datasets with induced artificial motion and on clinical datasets having complex motion. It should be noted that significant improvements are obtained from using our framework.

In what follows, Section 2 explains briefly the Demon's Deformable registration and its implementation in the National Library of Medicine NLM/NIH Segmentation and Registration Toolkit (ITK). Section 3 details our comparative evaluation study with results. Finally, we report our conclusions and outline our plans for the future in Section 4.

2 3D Elastic Co-registration: Thirion's Demons

Thirion [5, 6] introduced the concept of diffusing models to perform image matching, an essential component of this study. Image matching is performed through the movement of a deformable grid through a semi-permeable contour of an object surface in the other image. The idea is derived from an analogy of Maxwell's demons aiding the diffusion of fluid through a semi-permeable membrane. Validated results were presented with synthesized deformations on real medical images. The method was applied successfully to track heart-motion which is similar to the motion in DCE-MRI images. Additionally, the method was also applied to three-dimensional inter-patients matching of brain images [7] with different shapes and intensities. In [4], a study of evaluating the temporal variations of lesion volumes for practical applications such as therapeutic intervention effects, decision making for drug treatment and pharmaceutical trials was conducted. This places our work in perspective. We seek to apply Thirion's method to the co-registration of DCE-MRI images. Now, we describe the ITK implementation of the method.

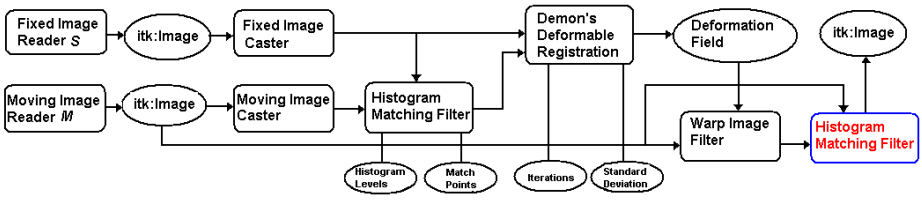

Fig. 2. ITK pipeline for the Demon's deformable registration

The input is a pair of stationary (S) and moving (M) images. Every object surface in S is defined by pixels on its boundary contour, also called demons.

The demons are responsible for applying force vectors on the deformable grid in M. Based on the location of the grid point in M with respect to the contours in S, the demons decide the polarity (direction) of the force vectors. Iteratively, the force created by the demons cause motion that is applied to the model. As the model draws closer to the contours (demons), the forces applied decreases gradually after each iteration. At convergence, the determined deformation field in M is applied to warp into S. For the DCE-MRI images, each of the epochs provides a $3D$ volume which is registered to a pre-determined base 3D volume.

Registration Framework Components The demons algorithm relies on the assumption that pixels representing the same geometric point on both the images have the same intensity on both the fixed and moving images to be registered. In DCE-MRI, there is a non-uniform uptake of the contrast medium affecting only the intensity in tissue pixels with the background being unaffected. Therefore, to obtain optimal results, we apply a itk::HistogramMatchingImageFilter. The parameters for this ITK filter include the histogram bins and the number of match points. The background pixels are eliminated during histogram computation in both the images by thresholding at the mean intensity. Hence, only those points affected by the contrast media are scaled back to the intensities in the base volume.

The itk::DemonsRegistrationFilter outputs a deformation field. The convergence is user-specified by the number of iterations. The deformation in each iteration is filtered by convolving with a Gaussian-kernel. Hence, the parameters in the deformation filter include the standard deviation of the Gaussian kernel, the interpolation method and the number of iterations. For DCE-MRI images, 50 iterations yielded optimal performance with the standard deviation set at 1.0. The itk::WarpImageFilter takes the final smoothed deformation field and the moving image as input and outputs a deformed image.

3 Enhancements and Results

We now present some results from the registration framework just described. Fifteen patients with eye tumors were included in the study protocol. DCE-MRI datasets were acquired on a clinical 1.5-T MR system (GE SIGNA) using a fast gradient-echo sequence (3D-FSPGR) with the following parameters: repetition time = 7.5 msec, echo time = 2.9 msec, flip angle = 25, FOV = 320, matrix size = 256 x 256, slice thickness = 3 mm, number of excitations = 0.5 using a standard phased array body coil. Total scan time was about 8 minutes. After the third phase a small molecular weight paramagnetic contrast agent (e.g. Gd-DTPA, Magnevist) was injected using a power injector at a constant infusion rate of 0.66 cc/s; dose 0.1 mmol/kg bodyweight for approximately $18s$. 3D volumes of the eye at 32 time-points were acquired with peak contrast being evident in the fifth time-point.

Figure 3 (A,B) shows two slice of the dataset extracted from the 3D volumes at fifth and tenth time-points. It is easy to observe that the slice B suffers from motion-induced warping. Image C is the difference image of A and B, clearly

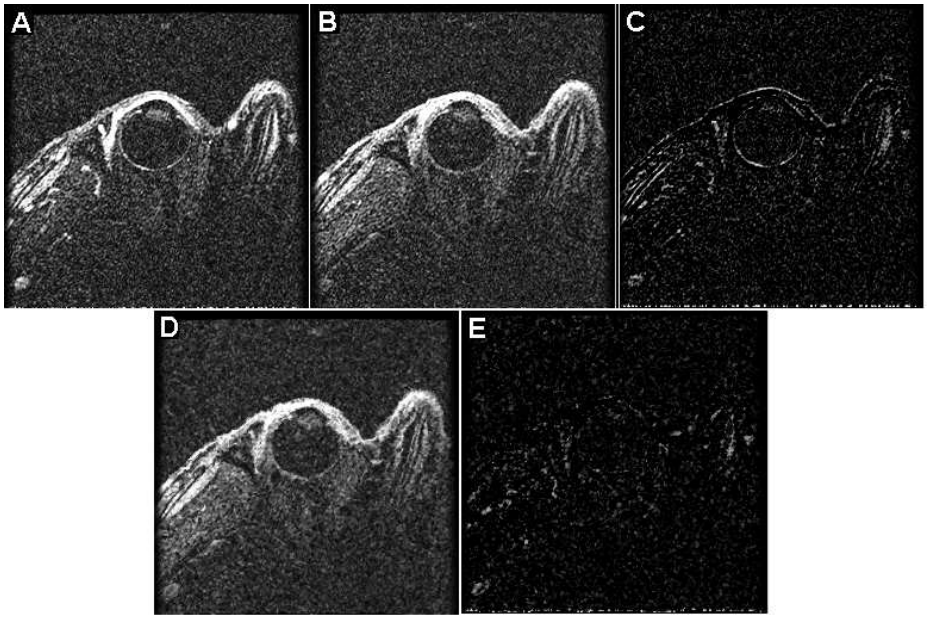

Fig. 3. A: Static slice. B: Motion-affected slice C: Difference image D: Slice B after registration E: Difference image after registration.

indicating the mis-alignment in boundaries. Co-registration of all the 32 volumes was done with the volume at the fifth time-point being considered as the fixed image. Image D is the slice extracted after the elastic registration of the 3D volume at tenth time-point. The difference image of D and A is shown in image E. The improvements and alignment of the boundaries in D are easy to observe over C.

Breast datasets were acquired using the similar study protocol. The breast was imaged in a pendant position and suffered elastic deformation. Twenty-six image volumes were acquired for analysis. Each volume was again registered to the volume at the fifth time-point. Figure 3 (A,B) show the volume renderings of the difference volumes at the twelfth time-point prior- and post-registration. Owing to misalignment in A, the tumor is covered by the breast tissue and does not permit visualization. In Figure 3 (B), however, we can clearly see the tumor morphology in 3D. Using the clustering approach in [8], we effectively segment the tumor (C) to observe its heterogeneity.

The two-compartment model estimation of the lesion parameters depends on the temporal intensity variation in the ROI. Earlier, we mentioned that registration results in the smoothing of the image due to the interpolation of the warped image onto a grid. The iterative nature of the process with the registration filter causes the monotonic decrease in average pixel intensities in the ROI. Further, we also smooth the deformation field with a gaussian filter to avoid unrealistic deformations. Therefore, the contours in the image are often blurred. For exam-

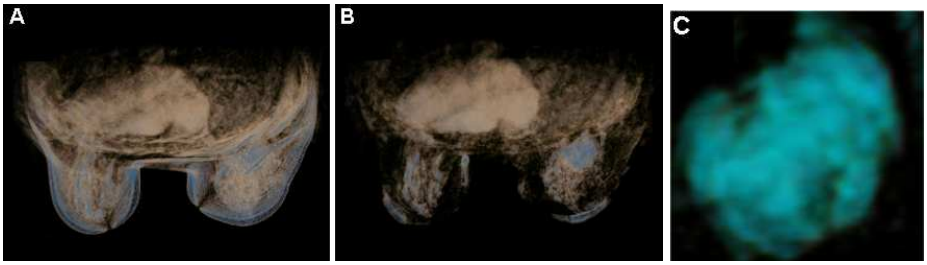

Fig. 4. A: 3D rendering using transfer functions of a difference volume B: 3D rendering of the difference volume after registration. C: Zoomed version of the tumor showing its heterogeneity

ple, Figure 3D shows the decrease in pixel intensities along with blurring in the registered eye dataset.

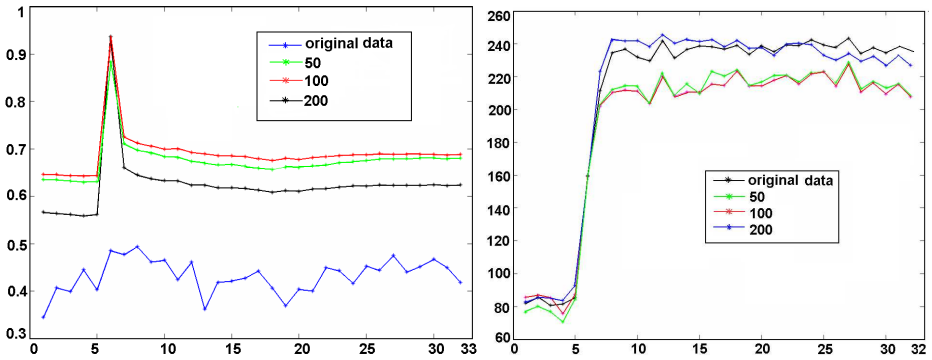

Fig. 5. Left: Pearson's correlation is plotted for each of the epochs after registration. Note that registration is carried out with the 5th epoch as the static dataset which causes the occurrence of a peak. Green, red and blue represent 50, 100 and 200 iterations respectively. The black line at the bottom represents the original volumes prior to registration. Right: Average ROI intensity plots after registration is complete. The black curve represents the true ROI intensities.

We now seek to understand registration on the basis of its affect on the pixel intensities. Datasets with motion cannot be chosen for validation purposes since there is no ground truth for pixel intensities after registration. For this purpose, DCE-MRI images of the eye with no motion in them are chosen. The data had 32 epochs and 24 slices with each slice being 256 x 256 in dimensions. Our task was complicated by the fact that the occurrence of such datasets is very rare.

We synthesize elastic motion in the volume by displacing each voxel based on its location with respect to 4 Gaussian functions namely, 1. time-point (4,10), 2. slice within the volume (8,10), 3. rotation angle (10°, 50) about the eye-center

and 4. constant translation of 20 vertically. The values in the brackets specify the mean and standard deviation of the applied Gaussian. The rationale behind this procedure is that deformation is smooth and continuous and may be represented as mixture of Gaussian kernels. The time-points tend to see a gradual increase and decrease in deformation. Further, the deformation in each time-point is maximum at a given slice and gradually declines for the neighboring slices. Such behavior is common in the case of elastic organs like the lung, liver and breast. The translation may be due to blood flow or regular breathing and can again be approximated as gaussian movements with large standard deviations. The standard deviations were chosen iteratively by a oncologist to reflect a real dataset found in practice. The deformed dataset is interpolated back onto a grid to represent a dataset with motion. The video sequence *deform.avi* attached shows a particular deformed slice across all time-points. Using the original and deformed datasets, we can evaluate the registration performance.

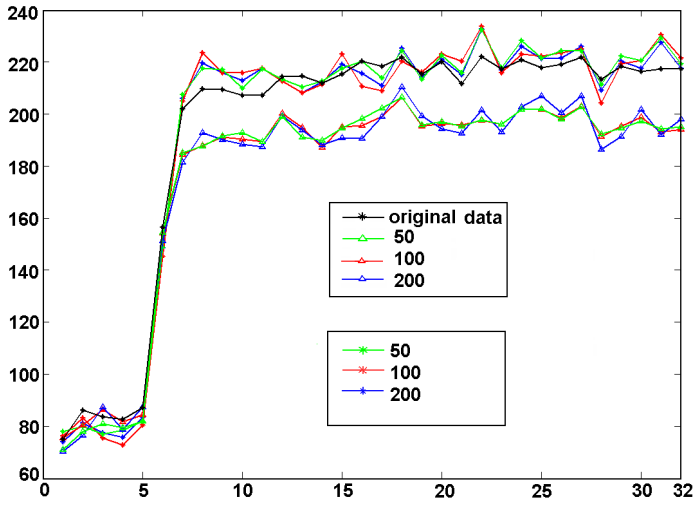

Fig. 6. The lower curves (red, blue and green with triangle markers) show the average ROI intensity in the registered volumes. The true ROI intensity is represented by the black curve. The set of upper curves (red, blue and green with star markers) represent the average ROI in registered volumes after doing a histogram matching for intensity correction. Note that these curves match the black curve closely. Green, red and blue represent 50, 100 and 200 iterations respectively.

Normally, registration methods have been evaluated on the basis of maximizing a similarity metric between two images. Using Pearson's formula, the correlation in the volumes prior to registration was 0.45 on average. After registration, the correlation was found to improve to 0.7 on average. Figure 5 (Left) shows the correlation of the eye dataset after registration. The blue line indi-

cates the correlation among the volumes prior to registration. The low values are partly due to the motion, white noise in the images and also from the continuous uptake and washout of the contrast medium. Registration improves the correlation significantly. The red, green and blue lines indicate the changing correlation values depending on the iterations of the registration algorithm. Longer iterative times tend to produce better registrations with diminishing returns progressively.

Figure 5 (Right) shows that as the registration accuracy improves (as a result of increased iteration), the drop in the average ROI intensity is more pronounced. Hence, we propose the use of a second itk::HistogramMatchingImageFilter after the registration is complete as shown in blue in Figure 2. Here, the reference image is the moving image M prior to registration. The histogram matching is done only in a region local to the ROI. This allows the non-linear scaling of the pixel intensities of the affected regions to match the original region. We also threshold using mean intensity value in order to eliminate the background voxels from interfering. Figure 6 shows the average ROI intensity plots after registration. The three lower curves (red, green and blue with triangle markers) are registered volumes without the histogram matching. The true ROI intensity curve is shown in black. After using the histogram matching filter, the registered volumes were scaled to match the black curve as shown by the red, green and blue curves with star markers. These curves lie in the vicinity of the black curve.

4 Conclusion and Future Work

In this paper, we described our experiences with using the Demon's co-registration method on DCE-MRI image sequences. We discuss the implementation of the Thirion's demon's 3D elastic registration method in the ITK framework. We evaluate the effectiveness of automatic co-registration on images with varying deformation, noise and registration parameter settings. We explore the effects of registration procedures on the pixel intensities and hence on the two-compartmental model quantified parameters. Hence, we incorporate ROI localized histogram-matching to obtain a suitable intensity mapping. In future, we will study the effects of different non-linear mapping strategies and conduct rigorous validation studies to establish a well-defined protocol for DCE-MRI image processing.

References

1. Knopp, M.V., Giesel, F.L., Marcos, H., Tengg-Kobligk, G., Choyke, P.: Dynamic contrast-enhanced magnetic resonance imaging in oncology. Top. Magn. Reso. Imaging **12** (2001) 301–308
2. Evelhoch, J.L.: Key factors in the acquisition of contrast kinetic data for oncology. J. Magn. Reson. Imaging **10** (2000) 254–259
3. Knopp, M.V., Weiss, E., Sinn, H.P., Mattern, J., Junkermann, H., Radeleff, J., Magener, A., Brix, D., Delorme, S., et al., I.Z.: Pathophysiologic basis of contrast enhancement in breast tumors. J. Magn. Reso. Imaging **10** (1999) 260–266

4. Thirion, J.P., Calmon, G.: Measuring lesion growth from 3D medical images. In: Nonrigid and Articulated Motion Workshop (NAM'97). (1997)
5. Thirion, J.P.: Fast non-rigid matching of 3D medical images. In: Medical Robotics and computer aided surgery, MRCAS'95. (1995) 47–54
6. Thirion, J.P.: Fast non-rigid matching of 3D medical images. In: Computer Vision and Pattern Recognition, CVPR'96. (1996)
7. Thirion, J.P., Subsol, G., Dean, D.: Cross validation of three inter-patients matching methods. In: Visualization in Biomedical Computing VBC'96, Lecture Notes in Computer Science. Volume 1131. (1996) 327–336
8. Rao, K., Machiraju, R., Heverhagen, J., Saltz, J., Knopp, M.: Exploratory segmentation using geometric tessellations (in presss). In: Proceedings of 10th International Fall Workshop on Vision, Modeling and Visualization. (2005)